

Cyclic Fatigue-Crack Growth and Fracture Properties in Ti_3SiC_2 Ceramics at Elevated Temperatures

Da Chen[†]

Department of Materials Science and Engineering, Shanghai Jiao Tong University, China

Kiroshi Shirato[†]

Department of Mechanical Engineering, Nagaoka University of Technology, Niigata, Japan

Michel W. Barsoum* and Tamer El-Raghy*

Department of Materials Engineering, Drexel University, Philadelphia, Pennsylvania 19104

Robert O. Ritchie

Materials Sciences Division, Lawrence Berkeley National Laboratory, and Department of Materials Science and Engineering, University of California, Berkeley, California 94720

The cyclic fatigue and fracture toughness behavior of reactive hot-pressed Ti_3SiC_2 ceramics was examined at temperatures from ambient to 1200°C with the objective of characterizing the high-temperature mechanisms controlling crack growth. Comparisons were made of two monolithic Ti_3SiC_2 materials with fine- (3–10 μm) and coarse-grained (70–300 μm) microstructures. Results indicate that fracture toughness values, derived from rising resistance-curve behavior, were significantly higher in the coarser-grained microstructure at both low and high temperatures; comparative behavior was seen under cyclic fatigue loading. In each microstructure, ΔK_{th} fatigue thresholds were found to be essentially unchanged between 25° and 1100°C; however, there was a sharp decrease in ΔK_{th} at 1200°C (above the plastic-to-brittle transition temperature), where significant high-temperature deformation and damage are first apparent. The substantially higher cyclic-crack growth resistance of the coarse-grained Ti_3SiC_2 microstructure was associated with extensive crack bridging behind the crack tip and a consequent tortuous crack path. The crack-tip shielding was found to result from both the bridging of entire grains and from deformation kinking and bridging of microlamellae within grains, the latter forming by delamination along the basal planes.

I. Introduction

THE ternary compound Ti_3SiC_2 exhibits a surprising combination of properties for a ceramic; e.g., it displays high toughness ($K_{\text{IC}} > 8 \text{ MPa}\cdot\text{m}^{1/2}$), a ratio of hardness ($\sim 4 \text{ GPa}$) to elastic modulus ($\sim 320 \text{ GPa}$) more typical of a ductile material, relatively low density (4.5 g/cm^3), and high resistance to thermal shock^{1,2}

and oxidation.³ Processed by reactive hot-pressing techniques from powders of titanium, SiC, and graphite, Ti_3SiC_2 also shows a range of inelastic deformation modes not typically seen in ceramics at room temperature,^{4–9} including grain bending, grain buckling, and significant amounts of basal slip. In general, Ti_3SiC_2 appears to be one of the most damage tolerant of all nontransforming monolithic ceramics.^{4–10}

The essential feature of the Ti_3SiC_2 structure is the relatively weak bonding between the silicon layer and the TiC octahedra, especially in shear, along the basal plane. Dislocations are mobile and multiply at room temperature. They are confined to two orthogonal directions: basal plane arrays (wherein the dislocations exist on identical slip planes) and walls or kink boundaries. Thus, in addition to regular slip, mechanisms for ambient temperature plastic deformation in Ti_3SiC_2 are thought to involve the readjustment of local stress and strain fields from kink band (boundaries) formation, buckling, and delamination of individual grains (the delamination and associated damage being contained by the kink boundaries).⁹ The delaminations typically occur at the intersection of the walls and arrays and result in the annihilation of the latter. It is this containment of damage that is believed to be a major source of damage tolerance in Ti_3SiC_2 . Specifically, delamination along the weaker basal planes leads to the creation of microlaminar structures contained within a single grain, the deformation and distortion of such laminae providing a potent contribution to toughening. In general, the plastic behavior seen in Ti_3SiC_2 is unusual for carbides and is believed to be caused by this layered structure and the metallic nature of the bonding.⁹

With such intrinsic deformation and toughness properties, Ti_3SiC_2 clearly offers some potential for many structural applications; however, if this is to be realized, it is important that some assessment be made of its subcritical crack-growth behavior. The fracture toughness and cyclic fatigue-crack growth behavior of monolithic Ti_3SiC_2 at ambient temperatures was first characterized by Gilbert *et al.*¹⁰ in both fine- (3–10 μm) and coarse-grained (50–200 μm) conditions. Fatigue-crack growth thresholds, ΔK_{th} , were found to be as high as 6 and 9 $\text{MPa}\cdot\text{m}^{1/2}$ in the fine- and coarse-grained structures, respectively; corresponding steady-state (plateau) resistance-curve (R-curve) fracture toughnesses, K_{IC} , were measured at 9.5 and 16 $\text{MPa}\cdot\text{m}^{1/2}$, respectively. The high toughness (the K_{IC} value for the coarse-grained structure is thought to be the highest ever reported for a monolithic, nontransforming ceramic) was found to be associated with a profusion of crack-bridging processes active in the crack wake. Indeed, Ti_3SiC_2

J. Rödel—contributing editor

Manuscript No. 188150. Received November 14, 2000; approved July 16, 2001. Supported by the Office of Science, Office of Basic Energy Sciences, Materials Sciences Division, U.S. Department of Energy (Contract No. DE-AC03-76SF00098) for the Berkeley group, and by the Army Research Office (DAAD19-00-1-0435) for the Drexel University group.

*Member, American Ceramic Society.

[†]Formerly of the Department of Materials Science & Engineering, University of California, Berkeley.

displayed a far larger degree of grain bridging and sliding^{6,7,10} than has been observed in other ceramics, such as Al_2O_3 , Si_3N_4 , and SiC ,^{11–13} possibly because the deformation processes observed in individual grains enhanced grain bridging by increasing pullout distances and suppressing grain rupture. Fatigue-crack growth, on the other hand, was associated with the cyclic loading induced degradation of such bridging; substantial evidence was found for wear degradation at active bridging sites behind the crack tip, particularly in the coarser-grained structure.

Although significant progress has been made in understanding the mechanical behavior of polycrystalline Ti_3SiC_2 at ambient temperatures, far less is understood about its properties at elevated temperatures. Its mechanical response in tension and creep up to 1200°C has been documented.^{14–17} The tensile response was found to be a strong function of strain rate and temperatures, and was characterized by a plastic-to-brittle transition[‡] (PBTT) at temperatures above 1150°C. Recently, Li *et al.*¹⁸ confirmed the ductile-to-brittle transition and showed that the Mode I fracture toughness (measured at 4.5 $\text{MPa}\cdot\text{m}^{1/2}$) was not only significantly lower than that measured at ambient temperature by Gilbert *et al.*,¹⁰ but that above 1273°C, the toughness decreased rapidly to $\sim 1/2$ its room temperature value. However, as far as we are aware, nothing is known about its cyclic fatigue-crack growth behavior and the R-curve properties at these elevated temperatures. It is the objective of the present paper to examine the mechanistic aspects of crack growth in Ti_3SiC_2 under both static and cyclic loading, in both fine- and coarse-grained microstructures, at temperatures from ambient to 1200°C, with the ultimate aim of defining the salient damage and crack-tip shielding mechanisms that govern the fracture toughness and cyclic fatigue-crack growth properties.

II. Experimental Procedure

(1) Material Processing and Microstructures

Ti_3SiC_2 specimens were fabricated by a reactive hot isostatic pressing technique using TiH_2 (−325 mesh, 99.99%), SiC (grain size $\sim 20\text{ }\mu\text{m}$, 99.5%), and graphite (grain size $\sim 1\text{ }\mu\text{m}$, 99%) starting powders. Powders with the desired stoichiometry were mixed in a ball mill, cold isostatically pressed at 200 MPa, and annealed at 900°C for 4 h *in vacuo* (10^{-3} Pa) to remove the hydrogen. Specimens were then sealed in glass under vacuum and hot isostatically pressed for 4 h at 1400° or 1600°C to form the

fine- and coarse-grained microstructures, respectively. The coarse-grained structure consisted of large plate-like grains of 70–300 μm diameter and 5–30 μm thickness, whereas grains in the fine-grained microstructure had a diameter of $\sim 7\text{ }\mu\text{m}$ and were $\sim 3\text{ }\mu\text{m}$ thick (Fig. 1). XRD and SEM showed that both structures contained $\sim 2\text{ vol}\%$ unreacted SiC . Further details on the procedures for fabricating Ti_3SiC_2 and its microstructural evolution have been reported elsewhere.^{1,2}

(2) Cyclic Fatigue Testing

Cyclic fatigue-crack growth tests were performed using 2.9 mm thick compact-tension C(T) specimens (of $\sim 19\text{ mm}$ width); this geometry conforms to the ASTM Standard E-647 for fatigue-crack growth rate measurements. Specimens were cycled at a constant load ratio (ratio of minimum to maximum applied loads) of $R = 0.1$ and a loading frequency of $\nu = 25\text{ Hz}$ (sinusoidal wave form), using automated stress-intensity K control. Growth rates were monitored under decreasing ΔK conditions with a normalized K -gradient ($1/K\cdot dK/da$) set to -0.08 mm^{-1} . Before testing, the C(T) samples were polished with $\sim 1\text{ }\mu\text{m}$ diamond paste and fatigue precracked at room temperature for several millimeters beyond the half-chevron-shaped starter notch. The latter notch geometry is used to facilitate crack initiation in brittle materials.

At elevated temperatures (1100° and 1200°C), testing was performed on a computer-controlled servo-hydraulic mechanical testing system in flowing gaseous argon at atmospheric pressure in an environmental chamber/furnace, heated by graphite elements that maintain temperature to within $\pm 1^\circ\text{C}$. Heating and cooling rates were kept at $10^\circ\text{C}/\text{min}$ to minimize any thermal shock effects. After reaching the desired temperature and before commencing the test, the furnace temperature was kept constant for 1–3 h to allow the system to reach thermal equilibrium.

At ambient temperatures, fatigue-crack growth rates were continuously measured using the standard back-face strain elastic-unloading compliance method, using a 350 Ω strain gauge affixed to the back surface of the specimen. This method could not be readily used at elevated temperatures; however, because Ti_3SiC_2 has good electrical conductivity at all temperatures, crack lengths at 1100° and 1200°C could be monitored *in situ* using the electrical-potential method. Full details of the use of electrical-potential methods for crack length monitoring in ceramics are given elsewhere.^{19,20} To verify such measurements at both ambient and elevated temperatures, readings were checked periodically using an optical microscope.

Cyclic fatigue-crack growth data are presented in terms of the growth rate per cycle, da/dN , as a function of the applied stress-intensity range, $\Delta K (= K_{\text{max}} - K_{\text{min}})$, the latter being computed using standard linear-elastic handbook solutions. Crack

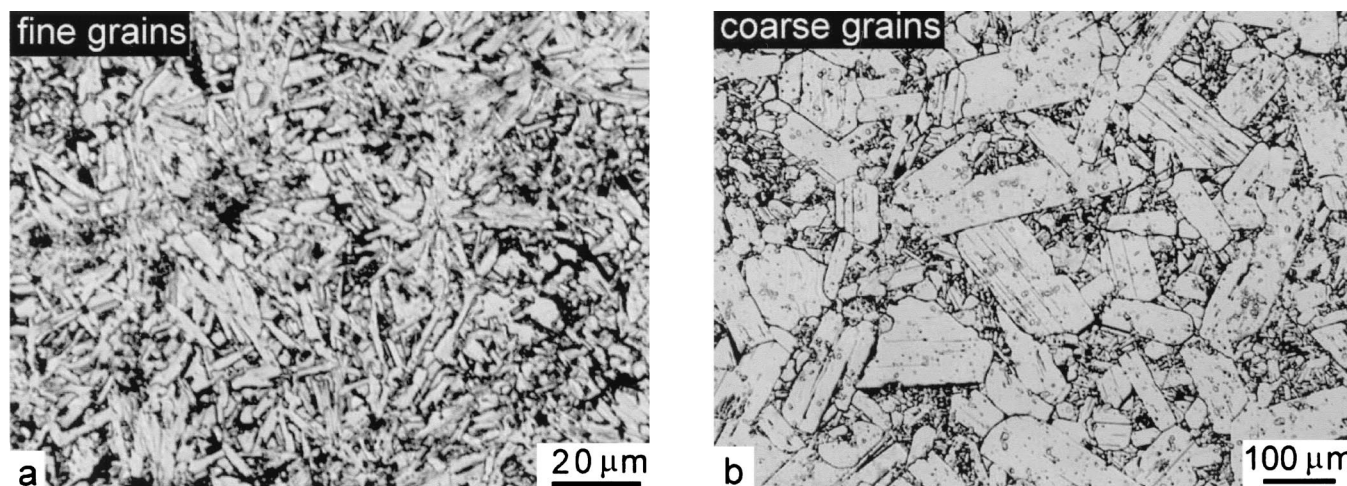


Fig. 1. Optical micrographs of the microstructures in Ti_3SiC_2 with (a) fine grains (3–10 μm) and (b) coarse grains (70–300 μm) etched in a 1:1:1 by volume $\text{HF}:\text{HNO}_3:\text{H}_2\text{O}$ solution. Note the layered nature of the grains, which is particularly evident in the coarse-grained structure.

[‡]The exact details of the plastic-to-brittle transition temperature (PBTT) are not understood at this time. It is fairly well-established, however, that it does not involve the activation of five or more independent slip systems,^{4,14–16} which is why we refer to the transition temperature as a PBTT instead of the more commonly used terminology of a ductile-to-brittle transition temperature.

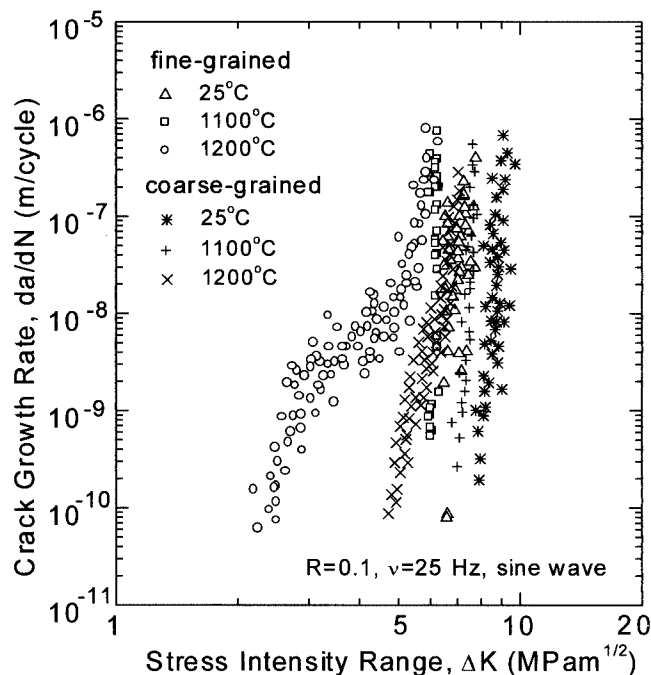


Fig. 2. Cyclic fatigue-crack growth rates, da/dN , at $R = 0.1$ and $\nu = 25$ Hz (sine wave) in Ti_3SiC_2 with fine- and coarse-grained microstructures, as a function of the applied stress-intensity range ΔK at temperatures of 25°, 1100°, and 1200°C.

profiles of selected fatigue samples, taken at midsection of the test piece perpendicular to the fracture surface, were examined with SEM.

(3) R-Curve Testing

Following completion of the fatigue tests, the R-curves were measured from the remaining uncracked portion of the specimens

by loading specimens to failure at elevated temperatures. Tests were conducted under displacement control by monotonically loading the C(T) specimens and monitoring subcritical crack growth using the electrical-potential method with periodic unloads of <10%. During the test, the applied load versus potential-drop curve was recorded for the further calculation of the R-curve. To minimize the effect of pre-existing crack-tip shielding on the measured initiation toughness from any grain bridging that may have developed during prior crack extension, before data collection, specimens were cycled at room temperature for ~24 h at the fatigue threshold, ΔK_{th} , and no crack extension was detected during this period.

III. Results and Discussion

(1) Cyclic Fatigue-Crack Growth Behavior

The variation in fatigue-crack growth rates, da/dN , with applied stress-intensity range, ΔK , in Ti_3SiC_2 at temperatures of 25°, 1100°, and 1200°C ($R = 0.1$, $\nu = 25$ Hz (sin wave)), is shown in Fig. 2 for the fine- and coarse-grained microstructures.

Characteristic of ceramic materials at low homologous temperatures,^{21,22} growth rates in both Ti_3SiC_2 microstructures at 25°C display a marked sensitivity to stress intensity. In terms of a simple Paris power-law expression, $da/dN \propto \Delta K^m$, the exponent m was measured to be between 72 and 85. Increasing the temperature to 1100°C results in only a small increase in growth rates, with fatigue thresholds reduced from ~8 to 7 $\text{MPa}\cdot\text{m}^{1/2}$ in the coarse-grained material, and from ~6.5 to 6 $\text{MPa}\cdot\text{m}^{1/2}$ in the fine-grained material; the slopes of the growth-rate curves remain essentially the same with $m \approx 79$ to 82.

However, at 1200°C, which is just above the PBTT of Ti_3SiC_2 ,^{4,14–18} the behavior is significantly different. Below $\sim 10^{-8}$ m/cycle, growth rates are substantially faster, the slope of the growth-rate curves are reduced, and there is a sharp decrease in the fatigue thresholds by a factor of ~2 and 3 $\text{MPa}\cdot\text{m}^{1/2}$ to ~2.3 and 4.5 $\text{MPa}\cdot\text{m}^{1/2}$ in both fine- and coarse-grained structures, respectively.

For many applications of structural materials, design must be based on the concept of a fatigue threshold ΔK_{th} for no crack

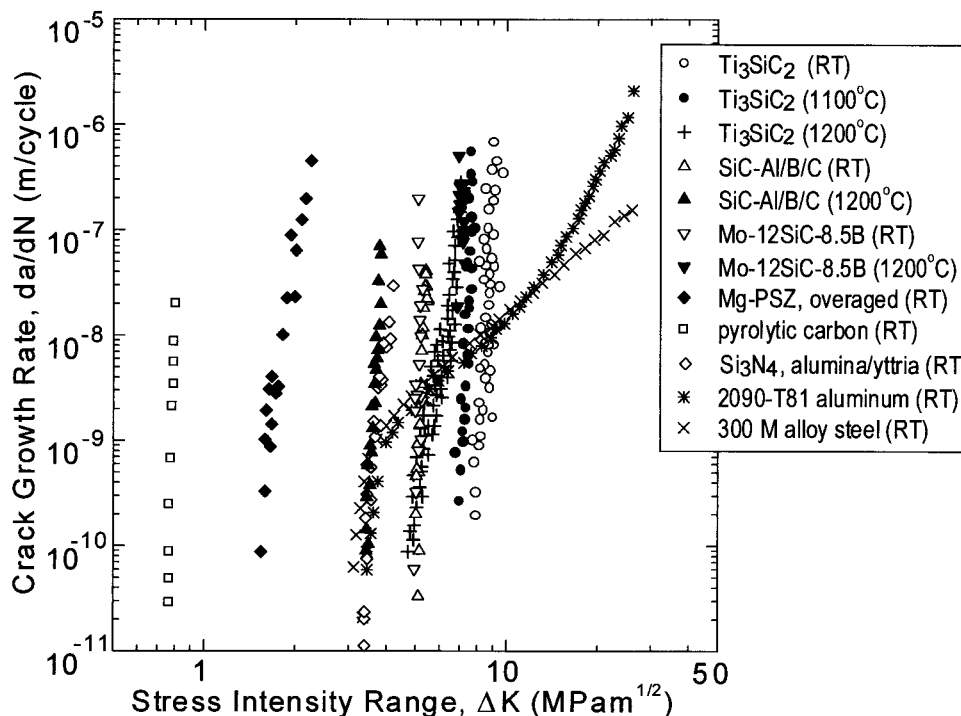


Fig. 3. Comparison of cyclic-fatigue properties of the coarse-grained Ti_3SiC_2 with behavior in a range of metals, intermetallics, and ceramics at both ambient and elevated temperatures.

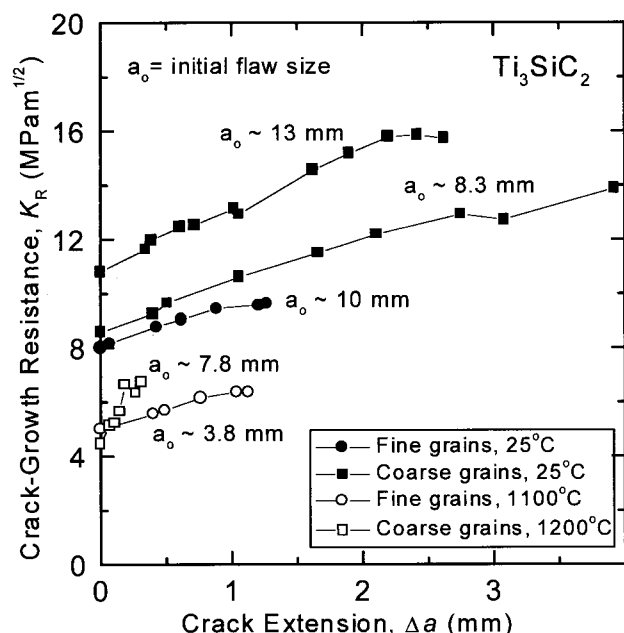


Fig. 4. Crack-growth resistance, K_R , is plotted as a function of crack extension, Δa , for both the fine- and coarse-grained Ti_3SiC_2 microstructures at ambient and elevated temperatures. The initial flaw size, a_0 , is indicated for each measured R-curve.

growth. Compared with more traditional structural ceramics, such as Si_3N_4 ,^{23–25} Al_2O_3 ,²⁶ and SiC ,²⁰ which have ΔK_{th} thresholds at 1000° to 1100°C of roughly 2 to 4 $\text{MPa}\cdot\text{m}^{1/2}$, depending on material and testing conditions, the cyclic fatigue properties of Ti_3SiC_2 (especially the coarse-grained microstructure) are clearly superior in terms of the fatigue threshold at both low and high temperatures. Indeed, at temperatures below its PBTT, Ti_3SiC_2 exhibits one of the highest fatigue thresholds and cyclic crack-growth resistances observed in a monolithic nontransforming ceramic or intermetallic. This is shown in Fig. 3 by a comparison of the cyclic-fatigue properties of the coarse-grained Ti_3SiC_2 with corresponding results in a range of metals, intermetallics, and ceramics at ambient and elevated temperatures.

(2) R-Curve Measurements

Substantial rising R-curves were measured in both fine- and coarse-grained Ti_3SiC_2 at both ambient and elevated temperatures (see Fig. 4). The R-curve for the fine-grained Ti_3SiC_2 rose in

increments of $\sim 1.6 \text{ MPa}\cdot\text{m}^{1/2}$ at 25°C and $\sim 1.4 \text{ MPa}\cdot\text{m}^{1/2}$ at 1100°C, to a steady-state toughness of roughly 10 and 6 $\text{MPa}\cdot\text{m}^{1/2}$, respectively. The corresponding coarse-grained Ti_3SiC_2 exhibited a more steeply rising R-curve with increments of ~ 4.9 to 5.3 $\text{MPa}\cdot\text{m}^{1/2}$ at 25°C and 2.3 $\text{MPa}\cdot\text{m}^{1/2}$ at 1200°C; maximum steady-state toughnesses for this structure were roughly 12–16 and 7 $\text{MPa}\cdot\text{m}^{1/2}$, respectively. It is clear that the crack-growth resistance of the coarse-grained microstructure is far superior to that of the fine-grained microstructure.

It should be noted that the initial flaw size, a_0 , appeared to affect the initial toughness, which is manifest as the starting point of the R-curve. This is considered to be associated with residual bridging in the fatigue precrack. As discussed below, there is significantly more bridging developed in the coarse-grained Ti_3SiC_2 structure, which exhibits a higher plateau toughness at both ambient and elevated temperatures. Crack paths in this microstructure were significantly more tortuous, and the lengths of bridging zones in the crack wake considerably larger, which are both factors that result in the development of the enhanced crack-wake bridging.

At 1200°C, i.e., above the PBTT of Ti_3SiC_2 , the coarse-grained microstructure still displays a rising R-curve, although the extent of stable crack growth is much reduced from ~ 3 to 4 mm at ambient temperatures to <0.5 mm at 1200°C. This is presumably caused by the onset of macro (creep) deformation of the specimen and, as discussed below, extensive microcracking at these elevated temperatures.

It is important to note that in contrast to most metallic and intermetallic solids for which the fracture toughness increases significantly above the PBTT, in Ti_3SiC_2 it drops. This is significant because it rules out the activation of additional slip systems as being the cause of the transition, which is in total accord with previous interpretations.^{4,14–17} The fact that it drops must therefore be related to a relaxation process ahead of the crack tip. It has recently been shown that creep and the tensile properties of Ti_3SiC_2 are dominated by such stress relaxation.^{15–17}

Currently, the exact mechanism for the relaxation is not well-understood, but is conjectured to result from an annealing out of dislocation pileups by a combination of delamination, microcracking, and/or grain boundary decohesion. The current work, while not proving these mechanisms exist, certainly supports their presence.

(3) Microstructural Characterizations

SEM images of the crack profiles during fatigue-crack growth at 25° and 1100°C in the coarse-grained microstructure are shown in Fig. 5. It is apparent that at 1100°C and below, i.e., below the PBTT, damage and shielding mechanisms are essentially unchanged from those at ambient temperatures. The fracture mode at

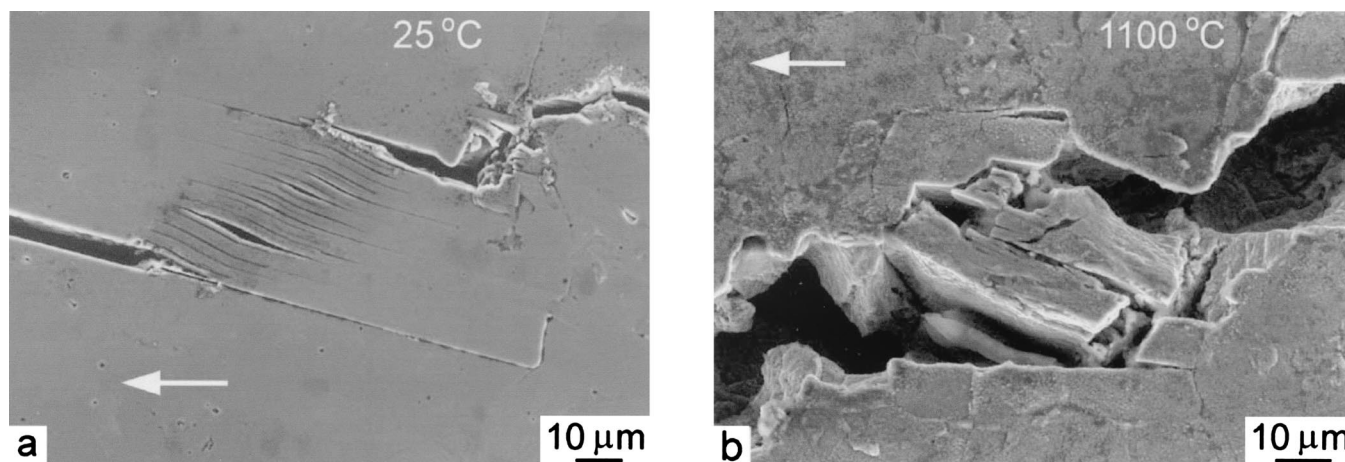


Fig. 5. SEM images of the profiles of fatigue cracks propagating at (a) 25°C and (b) 1100°C in the coarse-grained Ti_3SiC_2 microstructure. Note the crack-wake grain bridging at both temperatures, and the layered nature of the grains. Arrows indicate direction of crack growth.

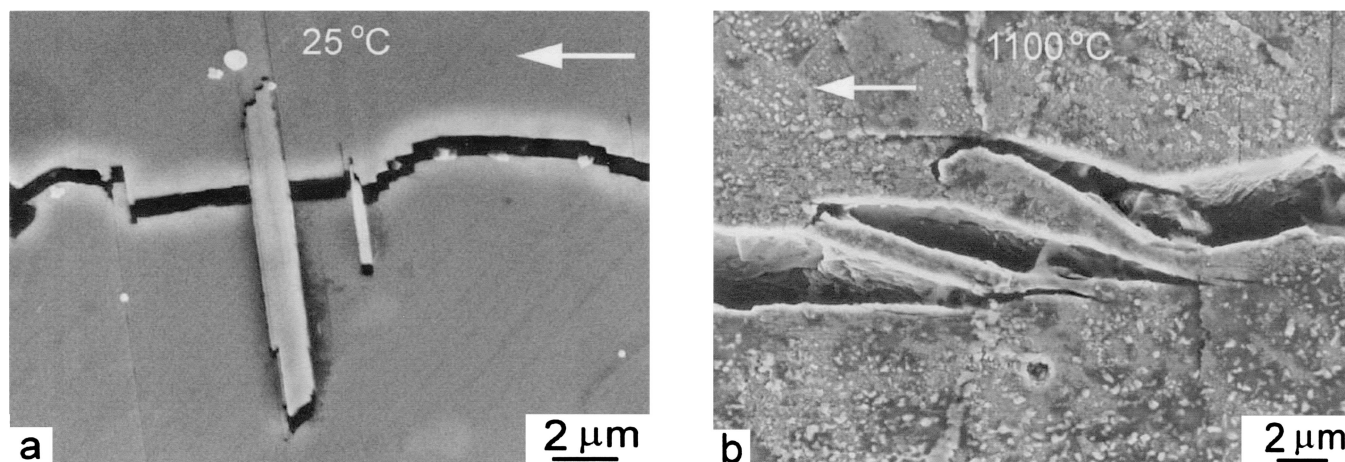


Fig. 6. SEM images of the profiles of fatigue cracks propagating at (a) 25°C and (b) 1100°C in the coarse-grained Ti_3SiC_2 microstructure, showing crack wake shielding by an individual or clusters of lamella within individual grains. Arrows indicate direction of crack growth.

both 25° and 1100°C is predominantly intergranular, or “interlamellar”, because of the delamination within the grains along the boundaries between the microlamellae (akin to a layered microstructure); moreover, ~10%–20% of the fracture surface consists of transgranular/“translamellar” cracking.

Similarly, the principal shielding mechanism in the crack wake remains grain bridging at both ambient and elevated temperatures. Specifically, wake shielding can be observed both in the form of bridged grains and their frictional pullout, and by an individual or clusters of lamella (typically deformed by bending) within individual grains (Fig. 6). This heavy deformation, together with the intrinsic strengths of the Ti–C bonds within the lamella,^{10,16} can increase the proportion of grains and lamellae participating in the bridging process, which acts to enlarge the extent of the bridging zone and, hence, increases the degree of toughening. Moreover, the bridging mechanisms associated with the lamellae appear to be particularly potent. Unlike other layered structures like mica and graphite, the debonding along the basal planes is bounded within a single grain and the resulting lamellae are quite flexible; the associated bending and kink band formation during deformation provides an ideal energy-absorbing microstructural feature to increase the resistance to crack growth. As this is not seen in more traditional ceramics, it presumably accounts for the superior damage tolerance shown by Ti_3SiC_2 .

Typically, grain bridging and frictional pullout constitute the major source of extrinsic toughening (i.e., crack-tip shielding) in monolithic ceramics, such as Si_3N_4 , Al_2O_3 , and SiC .¹² In Ti_3SiC_2 ,

the additional shielding process of the bending of deformed lamella appears to further enhance crack-growth resistance and, hence, the steady-state fracture toughness, by promoting very sizable bridging-zone lengths, which can exceed ~5 mm in the coarse-grained microstructure. Moreover, shear-faulting along the basal planes of the grain caused by sliding along the contacting surface of a bridge may also increase crack-growth resistance by reducing the severity of frictional damage in the layered microstructures.

Below the PBTT, which has been estimated to lie between 1100° and 1200°C,^{4,14–18} no noticeable evidence of extensive creep damage, in the form of microcracking zones and cavitation ahead of the crack tip or viscous-ligament bridging by a grain-boundary glassy phase in the wake, could be seen. As such, it is clear that the primary damage (intergranular and/or interlamellar cracking and the frictional wear degradation of the bridging zone in the crack wake) and crack-tip shielding (grain and lamellae bridging) mechanisms governing high-temperature fatigue-crack growth behavior in Ti_3SiC_2 up to ~1100°C, are essentially unchanged from those at ambient temperature.

The small decrease in crack-growth resistance at 1100°C (ΔK_{th} thresholds are ~8%–14% higher at 25°C) may be rationalized by considering the nature of grain bridging²⁷ and its degradation under cyclic loading caused by frictional wear.^{28,29} The pullout resistance from frictional tractions generated via sliding contact of opposing crack faces¹¹ is proportional to the normal stress acting on the interface, which, in turn, is a function of the residual stress

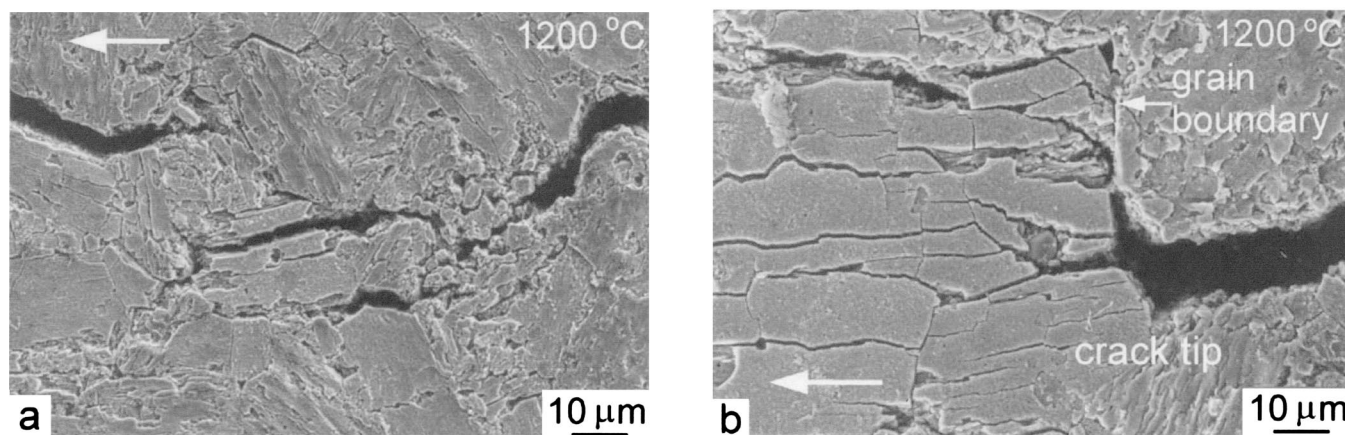


Fig. 7. SEM images of the profiles of fatigue cracks propagating at 1200°C, which is above the PBTT of Ti_3SiC_2 in the coarse-grained Ti_3SiC_2 microstructure: (a) crack-wake region and (b) crack-tip region. Note the profuse amounts of microcracks and cavities near the main crack. Arrows indicate direction of crack growth.

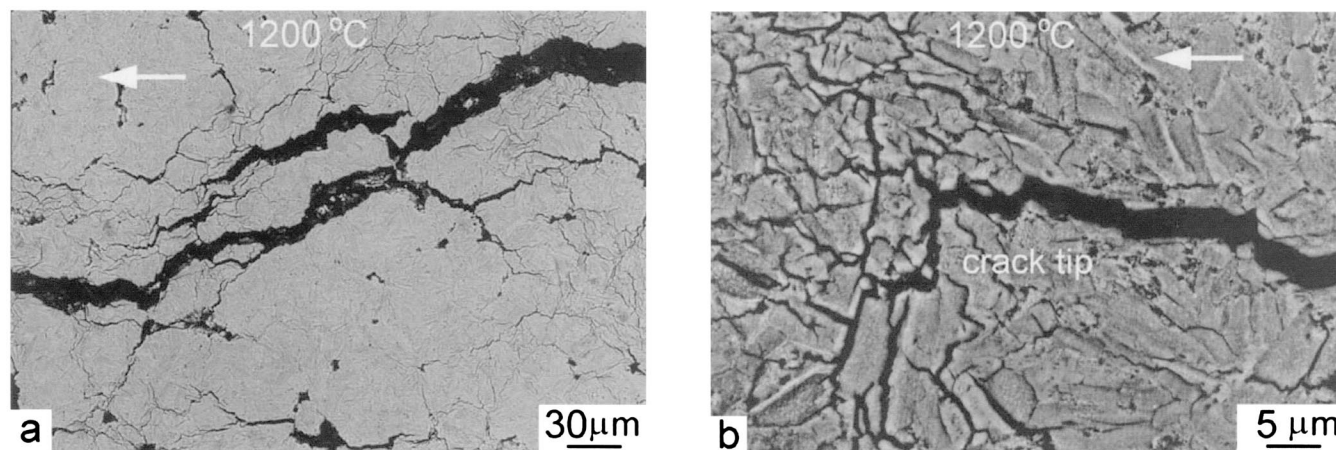


Fig. 8. SEM images of the profiles of fatigue cracks propagating at 1200°C in the fine-grained Ti_3SiC_2 microstructure: (a) crack-wake region and (b) crack-tip region. Note the profuse amounts of microcracks and cavities near the main crack. Arrows indicate direction of crack growth.

resulting from thermal expansion anisotropy during cooling from the processing temperature. As the residual stresses will “anneal out” with increasing temperature, the normal stress will decrease, thereby reducing the pullout resistance.

However, at 1200°C, above the PBTT, there is a striking change in behavior, principally in the form of significantly reduced ΔK_{th} thresholds that can be attributed to the onset of significant high-temperature deformation and associated microstructural damage. As noted above, at this temperature, macroscopic deformation of the test specimen was observed in the form of significant widening of the notch. More importantly, extensive microcracking and, to a lesser extent, cavitation, was apparent throughout the sample in both microstructures, although the intensity of damage was most severe in the vicinity of the crack tip. This is shown in Figs. 7 and 8 for coarse- and fine-grained microstructures, respectively. Moreover, crack paths involved significantly more transgranular and/or translamellar cracking, especially in the fine-grained microstructure, compared with that seen at lower temperatures, which severely diminished the propensity for grain bridging in the crack wake.

In summary, Ti_3SiC_2 represents an extremely damage-tolerant ceramic, with exceptional ambient temperature toughness and only a small degradation in fracture and fatigue properties at elevated temperatures below ~1100°C. Of the two structures examined, the coarse-grained microstructure displays a markedly higher K_{IC} fracture toughness and ΔK_{th} threshold at both low and high temperatures, principally resulting from substantially more tortuous crack paths and extensive crack-wake bridging because of much larger bridging zones, typically ~4–5 mm in length in the coarse-grained structures compared with less than ~200 µm in the fine-grained structure. However, the mechanical properties of this material degrade substantially at 1200°C above the PBTT because of the onset of significant high-temperature damage mechanisms, specifically, macroscopic (creep) deformation and extensive microcracking.

IV. Conclusions

Based on a study of cyclic fatigue-crack propagation behavior at elevated temperatures up to 1200°C in a reactively hot-pressed monolithic Ti_3SiC_2 ceramic with both fine- (3–10 µm) and coarse-grained (70–300 µm) microstructures, the following conclusions can be drawn:

(1) The cyclic fatigue-crack growth properties of Ti_3SiC_2 were found to be superior to those of more traditional monolithic (nontransforming) structural ceramics, such as Si_3N_4 , Al_2O_3 , and SiC, both at ambient and elevated temperatures up to ~1100°C. Compared with behavior at ambient temperature, fatigue thresholds were only reduced by between ~8% and 13% at 1100°C;

specifically, ΔK_{th} values were found to be ~6 and 7 $\text{MPa}\cdot\text{m}^{1/2}$ in the fine- and coarse-grained microstructures, respectively. In both structures and at all temperatures below ~1100°C, growth rates displayed a marked sensitivity to stress intensity, with Paris power-law exponents varying from $m \approx 72$ to 85.

(2) Mechanistically, damage and crack-tip shielding processes that were active at 1100°C were essentially unchanged from those at ambient temperature. Crack-path profiles showed a predominantly intergranular and/or interlamellar mode of crack advance with consequent crack-tip shielding by both grain and lamellae bridging in the crack wake. The lamellae bridging mechanism, associated with basal plane delaminations within single grains, appears to be a particularly potent source of toughening. As this is not seen in more traditional ceramics, it presumably accounts for the superior damage tolerance shown by Ti_3SiC_2 .

(3) At 1200°C, above the plastic-to-brittle transition temperature, a striking change in the shape of the growth-rate curves was observed with ΔK_{th} thresholds being severely reduced by a factor of ~2 and 3 to ~2.3 and 4.5 $\text{MPa}\cdot\text{m}^{1/2}$ in the fine- and coarse-grained microstructures, respectively. Such behavior was attributed to the onset of significant high-temperature damage, in the form of macroscopic deformation of the sample, the presence of widespread microcracking and cavity formation, and the onset of some degree of transgranular and translamellar cracking, which limited shielding by grain bridging in the crack wake.

(4) Substantial rising R-curves were measured in both fine- and coarse-grained Ti_3SiC_2 , and at both ambient and elevated temperatures with stable crack extensions between 0.5 and 4 mm.

(5) Higher (steady-state) R-curve fracture toughness and cyclic fatigue-crack growth resistance were achieved in the coarse-grained Ti_3SiC_2 microstructure at both low and elevated temperatures. Indeed, this microstructure exhibited ~15%–48% higher fatigue thresholds than the fine-grained microstructure at all temperatures between 25° and 1200°C. This is attributed to more extensive crack-wake bridging in the coarser structure in the form of larger bridging zones and a greater tortuosity in crack paths.

References

- ¹M. W. Barsoum and T. El-Raghy, “Synthesis and Characterization of a Remarkable Ceramic: Ti_3SiC_2 ,” *J. Am. Ceram. Soc.*, **79**, 1953–56 (1996).
- ²T. El-Raghy and M. W. Barsoum, “Processing and Mechanical Properties of Ti_3SiC_2 , Part I, Reaction Path and Microstructure Evolution,” *J. Am. Ceram. Soc.*, **82**, 2849–54 (1999).
- ³M. W. Barsoum, T. El-Raghy, and L. Ogbuji, “Oxidation of Ti_3SiC_2 in Air,” *J. Electrochem. Soc.*, **144**, 2508–16 (1997).
- ⁴T. El-Raghy, M. W. Barsoum, A. Zavaliangos, and S. Kalidindi, “Processing and Mechanical Properties of Ti_3SiC_2 , Part II, Effect of Grain Size and Deformation Temperature,” *J. Am. Ceram. Soc.*, **82**, 2855–60 (1999).
- ⁵M. W. Barsoum and T. El-Raghy, “Room-Temperature Ductile Carbides,” *Metall. Mater. Trans. A*, **30**, 363–69 (1999).

- ⁶T. El-Raghy, A. Zavaliangos, M. W. Barsoum, and S. R. Kalidindi, "Damage Mechanisms Around Hardness Indentations in Ti_3SiC_2 ," *J. Am. Ceram. Soc.*, **80**, 513–16 (1997).
- ⁷I. M. Low, S. K. Lee, B. R. Lawn, and M. W. Barsoum, "Contact Damage Accumulation in Ti_3SiC_2 ," *J. Am. Ceram. Soc.*, **81**, 225–28 (1998).
- ⁸L. Farber, M. W. Barsoum, A. Zavaliangos, and T. El-Raghy, "Dislocations and Stacking Faults in Ti_3SiC_2 ," *J. Am. Ceram. Soc.*, **81**, 1677–81 (1998).
- ⁹M. W. Barsoum, L. Farber, T. El-Raghy, and I. Levin, "Dislocations, Kink Bands and Room Temperature Plasticity of Ti_3SiC_2 ," *Metall. Mater. Trans. A*, **30**, 1727–38 (1999).
- ¹⁰C. J. Gilbert, D. R. Bloyer, M. W. Barsoum, T. El-Raghy, A. P. Tomsia, and R. O. Ritchie, "Fatigue-Crack Growth and Fracture Properties of Coarse and Fine-Grained Ti_3SiC_2 ," *Scr. Mater.*, **42**, 761–67 (2000).
- ¹¹P. L. Swanson, C. J. Fairbanks, B. R. Lawn, Y. W. Mai, and B. J. Hockey, "Crack-Interface Grain Bridging as a Fracture Resistance Mechanism in Ceramics: I, Experimental Study on Alumina," *J. Am. Ceram. Soc.*, **70**, 279–89 (1987).
- ¹²C. W. Li, D. J. Lee, and S. C. Lui, "R-curve Behavior and Strength for *In-Situ*-Reinforced Silicon Nitrides with Different Microstructures," *J. Am. Ceram. Soc.*, **75**, 1777–85 (1992).
- ¹³C. J. Gilbert and R. O. Ritchie, "On the Quantification of Bridging Traction during Subcritical Crack Growth under Monotonic and Cyclic Fatigue Loading in a Grain-Bridging Silicon Carbide Ceramic," *Acta Mater.*, **46**, 609–16 (1998).
- ¹⁴M. Radovic, M. W. Barsoum, T. El-Raghy, J. Seidensticker, and S. Wiederhorn, "Tensile Properties of Ti_3SiC_2 in the 25–1300°C Temperature Range," *Acta Mater.*, **48**, 453–59 (2000).
- ¹⁵M. Radovic, M. W. Barsoum, T. El-Raghy, S. Wiederhorn, and W. Luecke, "Effect of Temperature, Strain Rate and Grain Size on the Mechanical Response of Ti_3SiC_2 in Tension," *Acta Mater.*, in press.
- ¹⁶M. Radovic, M. W. Barsoum, T. El-Raghy, and S. Wiederhorn, "Tensile Creep of Fine-Grained (3–5 μm) Ti_3SiC_2 in the 1000–1200°C Temperature Range," *Acta Mater.*, in press.
- ¹⁷M. Radovic, M. W. Barsoum, T. El-Raghy, and S. Wiederhorn, "Tensile Creep of Coarse-Grained (100–300 μm) Ti_3SiC_2 in the 1000–1200°C Temperature Range," *Metall. Mater. Trans. A*, in press.
- ¹⁸J.-F. Li, W. Pan, F. Sato, and R. Watanabe, "Mechanical Properties of Polycrystalline Ti_3SiC_2 at Ambient and Elevated Temperatures," *Acta Mater.*, **49**, 937–45 (2001).
- ¹⁹D. Chen, C. J. Gilbert, and R. O. Ritchie, "In Situ Measurement of Fatigue Crack Growth Rates in a Silicon Carbide Ceramic at Elevated Temperatures Using a DC Potential System," *J. Test. Eval.*, **28**, 236–41 (2000).
- ²⁰D. Chen, C. J. Gilbert, X. F. Zhang, and R. O. Ritchie, "High-Temperature Cyclic Fatigue-Crack Growth Behavior in an *In Situ* Toughened Silicon Carbide," *Acta Mater.*, **48**, 659–74 (2000).
- ²¹R. O. Ritchie and R. H. Dauskardt, "Cyclic Fatigue in Ceramics: A Fracture Mechanics Approach to Subcritical Crack Growth and Life Prediction," *J. Ceram. Soc. Jpn.*, **99**, 1047–62 (1991).
- ²²C. J. Gilbert and R. O. Ritchie, "Mechanisms of Cyclic Fatigue-Crack Propagation in a Fine-Grained Alumina Ceramic: Role of Crack Closure," *Fatigue Fract. Eng. Mater. Struct.*, **20**, 1453–66 (1997).
- ²³Y. H. Zhang and L. Edwards, "Cyclic Fatigue Crack Growth Behavior of Silicon Nitride at 1400°C," *Mater. Sci. Eng., A*, **256**, 144–51 (1998).
- ²⁴S.-Y. Liu, I.-W. Chen, and T.-Y. Tien, "Fatigue Crack Growth of Silicon Nitride at 1400°C: A Novel Fatigue-Induced Crack-tip Bridging Phenomenon," *J. Am. Ceram. Soc.*, **77**, 137–42 (1994).
- ²⁵U. Ramamurty, T. Hansson, and S. Suresh, "High-Temperature Crack Growth in Monolithic and SiC_w -Reinforced Silicon Nitride under Static and Cyclic Loads," *J. Am. Ceram. Soc.*, **77**, 2985–99 (1994).
- ²⁶L. Ewart and S. Suresh, "Elevated-Temperature Crack Growth in Polycrystalline Alumina under Static and Cyclic Loads," *J. Mater. Sci.*, **27**, 5181–91 (1992).
- ²⁷B. R. Lawn, *Fracture of Brittle Solids*, 2nd ed. Cambridge University Press, New York, 1993.
- ²⁸S. Lathabai, J. Rödel, and B. R. Lawn, "Cyclic Fatigue from Frictional Degradation at Bridging Grains in Alumina," *J. Am. Ceram. Soc.*, **74**, 1340–48 (1991).
- ²⁹R. H. Dauskardt, "A Frictional-Wear Mechanism for Fatigue-Crack Growth in Grain Bridging Ceramics," *Acta Metall. Mater.*, **41**, 2765–81 (1993). □